

## Article

# In Situ SERS Sensing by a Laser-Induced Aggregation of Silver Nanoparticles Templated on a Thermoresponsive Polymer

Larisa V. Sigolaeva <sup>1,\*</sup> , Natalia L. Nechaeva <sup>2</sup>, Anton I. Ignatov <sup>3,4</sup>, Lyubov Y. Filatova <sup>1</sup> , Timur Z. Sharifullin <sup>1</sup> , Jonas Eichhorn <sup>5</sup>, Felix H. Schacher <sup>5,6,7</sup> , Dmitry V. Pergushov <sup>1,8</sup> , Alexander M. Merzlikin <sup>9</sup> and Ilya N. Kurochkin <sup>1,2,\*</sup>

<sup>1</sup> Department of Chemistry, M.V. Lomonosov Moscow State University, 119991 Moscow, Russia

<sup>2</sup> N.M. Emanuel Institute of Biochemical Physics of Russian Academy of Sciences, 119334 Moscow, Russia

<sup>3</sup> All-Russia Research Institute of Automatics, 127055 Moscow, Russia

<sup>4</sup> National Research Moscow State University of Civil Engineering, 129337 Moscow, Russia

<sup>5</sup> Institute of Organic Chemistry and Macromolecular Chemistry (IOMC), Friedrich-Schiller-University Jena, D-07743 Jena, Germany

<sup>6</sup> Jena Center for Soft Matter (JCSM), Friedrich-Schiller-University Jena, D-07743 Jena, Germany

<sup>7</sup> Center for Energy and Environmental Chemistry (CEEC), Friedrich-Schiller-University Jena, D-07743 Jena, Germany

<sup>8</sup> N.N. Semenov Federal Research Center of Chemical Physics of Russian Academy of Sciences, 119991 Moscow, Russia

<sup>9</sup> Institute of Theoretical and Applied Electromagnetics of Russian Academy of Sciences, 125412 Moscow, Russia

\* Correspondence: lsigolaeva@belozersky.msu.ru (L.V.S.); ikur@sky.chph.ras.ru (I.N.K.); Tel.: +7-495-939-40-42 (L.V.S.); +7-495-939-43-91 (I.N.K.)



**Citation:** Sigolaeva, L.V.; Nechaeva, N.L.; Ignatov, A.I.; Filatova, L.Y.; Sharifullin, T.Z.; Eichhorn, J.; Schacher, F.H.; Pergushov, D.V.; Merzlikin, A.M.; Kurochkin, I.N. In Situ SERS Sensing by a Laser-Induced Aggregation of Silver Nanoparticles Templated on a Thermoresponsive Polymer. *Biosensors* **2022**, *12*, 628. <https://doi.org/10.3390/bios12080628>

Received: 16 June 2022

Accepted: 5 August 2022

Published: 11 August 2022

**Publisher's Note:** MDPI stays neutral with regard to jurisdictional claims in published maps and institutional affiliations.



**Copyright:** © 2022 by the authors. Licensee MDPI, Basel, Switzerland. This article is an open access article distributed under the terms and conditions of the Creative Commons Attribution (CC BY) license (<https://creativecommons.org/licenses/by/4.0/>).

**Abstract:** A stimuli-responsive (pH- and thermoresponsive) micelle-forming diblock copolymer, poly(1,2-butadiene)<sub>290</sub>-*block*-poly(*N,N*-dimethylaminoethyl methacrylate)<sub>240</sub> (PB-*b*-PDMAEMA), was used as a polymer template for the in situ synthesis of silver nanoparticles (AgNPs) through Ag<sup>+</sup> complexation with PDMAEMA blocks, followed by the reduction of the bound Ag<sup>+</sup> with sodium borohydride. A successful synthesis of the AgNPs on a PB-*b*-PDMAEMA micellar template was confirmed by means of UV-Vis spectroscopy and transmission electron microscopy, wherein the shape and size of the AgNPs were determined. A phase transition of the polymer matrix in the AgNPs/PB-*b*-PDMAEMA metallopolymer hybrids, which results from a collapse and aggregation of PDMAEMA blocks, was manifested by changes in the transmittance of their aqueous solutions as a function of temperature. A SERS reporting probe, 4-mercaptophenylboronic acid (4-MPBA), was used to demonstrate a laser-induced enhancement of the SERS signal observed under constant laser irradiation. The local heating of the AgNPs/PB-*b*-PDMAEMA sample in the laser spot is thought to be responsible for the triggered SERS effect, which is caused by the approaching of AgNPs and the generation of “hot spots” under a thermo-induced collapse and the aggregation of the PDMAEMA blocks of the polymer matrix. The triggered SERS effect depends on the time of a laser exposure and on the concentration of 4-MPBA. Possible mechanisms of the laser-induced heating for the AgNPs/PB-*b*-PDMAEMA metallopolymer hybrids are discussed.

**Keywords:** thermoresponsive; silver nanoparticles; SERS; 4-mercaptophenylboronic acid; amphiphilic diblock copolymer; poly(*N,N*-dimethylaminoethyl methacrylate); laser-induced aggregation; plasmonic heating; local laser exposure

## 1. Introduction

Surface-enhanced Raman scattering (SERS) is an ultrasensitive vibrational spectroscopic technique, which aims to detect analytes in close proximity to a surface of plasmonic nanostructures. It is now well understood that the plasmonic coupling effect among

particles induces enormous electromagnetic enhancement that allows SERS signals to be detected with very high or even single-molecule sensitivity [1,2].

Tremendous progress in fabricating nanostructured surfaces as SERS substrates, such as ordered arrays, fractal films, metal clusters, or colloidal metal nanoparticles (NPs), has taken place due to the intensive development of nanotechnology [3,4]. In addition to the ordering of micro- or nanostructures, the distance dependence of the enhancement effect has also been reported, including the effects of the distance between adjacent nanostructures and of the distance between analyte molecules and SERS substrate. The higher surface enhancement factors show a near exponential decay with the gap distance between NPs [5].

SERS-responsive assemblies of gold or silver nanoparticles (AuNPs or AgNPs) can be formed in situ, wherein the overall dimensions and interparticle spatial distances can respond and adapt to external stimuli. Importantly, the significant enhancement of SERS spectra arises from the compulsory aggregation of AuNPs or AgNPs, leading to the formation of “hot spots” in the gap between NPs. The aggregation of NPs can be achieved by increasing the ionic strength [6], ultrasound treatment [7], or application of gradient electric field [8].

Several research groups have reported on AuNPs or AgNPs associated with a thermosensitive polymer, that is, poly(*N*-isopropylacrylamide) (PNIPAAm). These new hybrid metallopolymer materials provide a controllable spatial distribution of metal NPs in the polymer matrix via temperature variation [9–11] as PNIPAAm undergoes a volume phase transition from a swollen hydrated state to a shrunken collapsed state when the temperature rises above 32 °C—a lower critical solution temperature (LCST) [12]. The temperature-controlled changes in the interparticle distances and the spatial distribution of the metal NPs in thermoresponsive PNIPAAm-based metallopolymer hybrid systems considerably enhanced the SERS sensing of 4-mercaptobenzoic acid [13], 1-naphthol [14,15], dyes [16–18], or biologically relevant molecules such as L-tyrosine or DNA [18].

An alternative to the external heating of temperature-sensitive metallopolymer hybrids would be laser-induced local heating, which would result in the spatial approaching of metal NPs, thereby enhancing the SERS signal. A phenomenon of microscopically observed phase transition was already previously described [19,20], wherein the microparticles of collapsed PNIPAAm were formed under direct heating with a focused infrared laser within 10–700 s [19] in aqueous solutions, depending on the polymer concentration, molecular weight of the polymer, temperature, or laser power. Furthermore, the localized surface plasmon resonance of single AuNPs attached to a transparent substrate can monitor the phase transition of PNIPAAm in aqueous solution upon a laser exposure [21]. Additionally, the local laser-induced plasmonic heating of AgNPs in the thermoresponsive dextran-grafted PNIPAAm copolymer/AgNPs hybrid system has been observed [22]. Worth noting, however, is that such local SERS triggering effects in temperature-sensitive metallopolymer hybrids have not been exploited for SERS sensing applications to date.

Poly(*N,N*-dimethylaminoethyl methacrylate) (PDMAEMA) is also classified as a thermoresponsive polymer. Its LCST is dependent on the pH of the surrounding aqueous medium [23,24], thereby rendering this polymer dual-stimuli-sensitive. Thus, the hydrophilic–hydrophobic balance of PDMAEMA can be changed by varying both the pH and temperature. Linear PDMAEMAs and PDMAEMA-based diblock copolymers have been used as efficient surface modifiers for the design of various types of electrochemical sensors, e.g., for choline [25–27], phenol [28], myoglobin [29], dsDNA [30,31], and drugs [32], as well as to reveal drug–DNA interactions [33]. PDMAEMA-based (co/ter)polymers were applied for the non-viral delivery of genetic material into cells [34,35]. PDMAEMA-based polymers were also reported as proper polymeric templates for the synthesis of metal NPs [36,37], wherein a strong stabilizing effect of PDMAEMA segments was reported [38].

In this work, we prepared metallopolymer hybrids consisting of AgNPs, which were templated on a poly(1,2-butadiene)<sub>290</sub>-*block*-poly(*N,N*-dimethylaminoethyl methacrylate)<sub>240</sub> (PB-*b*-PDMAEMA) diblock copolymer (where the subscripts denote the number-average de-

degrees of polymerization of the corresponding blocks). Apart from that, for the first time, we demonstrated local laser-induced enhancement of the SERS signal of 4-mercaptophenylboronic acid (4-MPBA) contacting with the obtained metallopolymer hybrid. Indeed, the possible local plasmonic heating of the AgNPs on PDMAEMA segments of the diblock copolymer under a laser irradiation might result in the heating of the polymer matrix in the laser spot and consequently initiate its phase transition (coil-to-globule transition of PDMAEMA segments followed by their subsequent aggregation). As assumed, the latter induces the approaching of AgNPs and thereby leads to the generation of “hot spots”. We also show herein that such a SERS triggering effect depends on the time of the laser exposure and on the concentration of 4-MPBA. Thus, we highlight a new approach to a SERS analysis that could imply potential applications in areas such as nanosensors for the detection and quantification of biologically relevant molecules.

## 2. Materials and Methods

### 2.1. Materials

4-MPBA, AgNO<sub>3</sub>, and NaBH<sub>4</sub> were obtained from Sigma-Aldrich. The PB-*b*-PDMAEMA diblock copolymer was synthesized as described earlier [29]. All other chemicals were of analytical grade and used without further purification. All aqueous solutions were prepared using Milli-Q water (18.2 MΩ·cm) purified with a Milli-Q water purification system by Millipore.

### 2.2. Polymer-Templated Synthesis of AgNPs

For the synthesis of an AgNPs/PB-*b*-PDMAEMA sample, an aqueous solution of AgNO<sub>3</sub> (24 μL, 0.1447 M) was first added to an alkaline solution of the PB-*b*-PDMAEMA diblock copolymer (3 mL, 0.023 M with respect to the monomer units of the polymer) at a Ag:N molar ratio of 1:20. The pH value of the mixture was carefully adjusted to pH 9 and the mixture was allowed to stay under stirring at room temperature for 30 min. Then, an aqueous solution of NaBH<sub>4</sub> (130 μL, 2 g/L) was added into the mixture to provide a NaBH<sub>4</sub>:AgNO<sub>3</sub> molar ratio of 2:1. Afterwards, the reaction mixture was stirred for 30 min at room temperature.

### 2.3. UV-Vis Spectroscopy

UV-Vis spectra were recorded using a Shimadzu UV-1800 double-beam spectrophotometer (Shimadzu, Kyoto, Japan) in quartz cuvettes with an optical path length of 10 mm. The spectra were acquired from 200 to 800 nm with a 1 nm resolution. Before acquisition, an AgNPs/PB-*b*-PDMAEMA sample was diluted 10 times with deionized water. The spectral data were treated with the ORIGIN software.

### 2.4. Transmission Electron Microscopy (TEM)

For TEM measurements, copper grids were rendered hydrophilic by Ar plasma cleaning for 2 min (Diener Electronics, Ebhausen, Germany). Ten microliters (10 μL) of either AgNPs/PB-*b*-PDMAEMA sample or control sample (AgNPs prepared in the absence of the PB-*b*-PDMAEMA diblock copolymer) were applied onto the grid and an excess of the sample was blotted with a filter paper. TEM images were acquired with a 200 kV FEI Tecnai G2 20 transmission electron microscope equipped with a 4 k × 4 k Eagle HS CCD and a 1 k × 1 k Olympus MegaView camera for overview images.

### 2.5. Turbidimetry

The transmittance of aqueous solutions of the PB-*b*-PDMAEMA diblock copolymer or aqueous dispersions of the AgNPs/PB-*b*-PDMAEMA metallopolymer hybrids with a concentration of 0.2 g/L (pH 9) was measured on a Shimadzu UV-1800 double-beam spectrophotometer (Shimadzu, Kyoto, Japan). The temperature-controlled sample holders were connected to a temperature controller allowing 6 simultaneous measurements. The samples were scanned at a fixed wavelength of 500 nm. Their light transmittance was recorded upon heating at a temperature variation rate of 0.4 °C/min. The inflection

points on the transmittance–temperature curves, which correspond to the onset temperature of the transmittance decrease, are defined herein as the onset temperature of phase transition ( $T_{PT}$ ).

### 2.6. Raman Spectroscopy

An SERS signal was measured using an innoRam Raman spectrometer (BWTek, Plainsboro, NJ, USA) with a laser wavelength of 532 nm and power of 40 mW. The SERS-active analyte, that is, 4-MPBA, was used as a reporter as this compound can covalently bind to the Ag surface due to its mercapto group. Aqueous solutions of 4-MPBA were prepared at the concentrations of 3, 6, 15, and 30  $\mu\text{M}$  and then mixed with an AgNPs/PB-*b*-PDMAEMA sample in a 1:1 ratio. Afterwards, the prepared mixtures were left for 30 min. Then, a 10  $\mu\text{L}$  aliquot of each mixture was applied onto aluminum foil. The SERS spectra were recorded in between 5–8 cycles of continuous laser exposition (each of 1 min duration). The acquisition time was 10 s. The characteristic peak of 4-MPBA at 1070  $\text{cm}^{-1}$  was used as an analytical signal for the evaluation of the SERS efficiency.

## 3. Results and Discussion

### 3.1. Physico-Chemical Characterization of the AgNPs Templated on the PB-*b*-PDMAEMA Micelles

In the present study, we used a stimuli-responsive (pH- and thermoresponsive) PB-*b*-PDMAEMA diblock copolymer, which comprises both a hydrophobic poly(1,2-butadiene) (PB) block with a low glass transition temperature ( $T_g$ ) of  $-15\text{ }^\circ\text{C}$  and a hydrophilic (chargeable) poly(*N,N*-dimethylaminoethyl methacrylate) (PDMAEMA) block. The chemical structure of the PB-*b*-PDMAEMA diblock copolymer is shown in Figure S1A.

The stimuli-responsiveness of the PB-*b*-PDMAEMA diblock copolymer results from the presence of a PDMAEMA block. PDMAEMA is a weak polybase with each monomer unit containing a pendant tertiary amino group. A reversible protonation of such amino groups imparts pH sensitivity to the PB-*b*-PDMAEMA diblock copolymer. According to the published results [29,32], PDMAEMA undergoes a transition from the fully protonated (charged) state to the fully deprotonated (non-charged) state in a pH window of 4.0–8.5, and the  $\text{pK}_a^{\text{app}}$  (at  $\alpha = 0.5$ , where  $\alpha$  is the degree of protonation of PDMAEMA) for the PB-*b*-PDMAEMA diblock copolymer was found to be 6.35. PDMAEMA is also related to thermosensitive polymers with cloud points of its aqueous solutions depending on the pH [23,24]. It is worth noting that the decreasing pH, which results in the charging of PDMAEMA due to the protonation of its monomer units, is accompanied by an increase in cloud points.

Being amphiphilic, the PB-*b*-PDMAEMA diblock copolymer self-assembles into micelles, which at the ambient temperature and neutral pH ( $\alpha = 0.75$ ) possess an overall average diameter of 106 nm. The micellar structure of the diblock copolymer was confirmed by means of cryogenic TEM (Figure S1B). Within a micelle, a hydrophobic PB core has a mean diameter of 38 nm while a hydrophilic PDMAEMA corona has a thickness of  $>34\text{ nm}$  [29]. The latter grants the formed PB-*b*-PDMAEMA micelles sufficient colloidal stability in aqueous media.

The in situ synthesis of AgNPs was performed by the pre-complexation of  $\text{Ag}^+$  ions with PDMAEMA blocks of the PB-*b*-PDMAEMA diblock copolymer, followed by their reduction to metallic Ag by sodium borohydride. The reduction was carried out at pH 9 by mixing an aqueous solution of  $\text{AgNO}_3$  with an aqueous solution of the PB-*b*-PDMAEMA micelles. The molar ratio of amino groups of PDMAEMA to  $\text{AgNO}_3$  (N:Ag) was kept at 20:1. According to our previously published results [25,29], all monomer units of PDMAEMA are uncharged ( $\alpha = 0$ ) at pH 9. Hence, the formation of an ion-coordination bond between an  $\text{Ag}^+$  ion and an uncharged N atom of a monomer unit of PDMAEMA was expected. The following reduction of  $\text{Ag}^+$  ions by a 2 molar excess of sodium borohydride results in the immediate appearance of a yellow-orange color, which indicates the formation of the AgNPs.

Figure 1A,B shows the UV–Vis spectra of the AgNPs formed in situ in the presence and in the absence of the PB-*b*-PDMAEMA diblock copolymer. As one can see, both samples, when freshly prepared, exhibit a characteristic surface plasmon resonance band at approximately 410–420 nm. While its position weakly depends on the presence or the absence of the copolymer, a considerable stabilization effect of the PB-*b*-PDMAEMA micelles is obvious. A spontaneous aggregation of non-stabilized AgNPs in the control sample results in a fast absorbance intensity decrease and broadening of the plasmonic peak soon after the preparation of AgNPs (Figure 1B). In solutions of the PB-*b*-PDMAEMA micelles, the plasmonic peak of the AgNPs keeps its position as well as its intensity (Figure 1A). One only notes certain (up and down) absorbance intensity variations for the metallopolymer hybrid system, which takes place during the first few days (Figure 1A). Afterwards, its absorbance demonstrates nearly no changes over at least 6 months (data not shown). The well-known strong stabilization effect of the PDMAEMA [38] is expected to impart such high colloidal stability to the AgNPs/PB-*b*-PDMAEMA metallopolymer hybrids. Apparently, the micellar structure of the PB-*b*-PDMAEMA diblock copolymer (Figure S1) could additionally contribute to the enhanced colloidal stability of the AgNPs/PB-*b*-PDMAEMA samples.

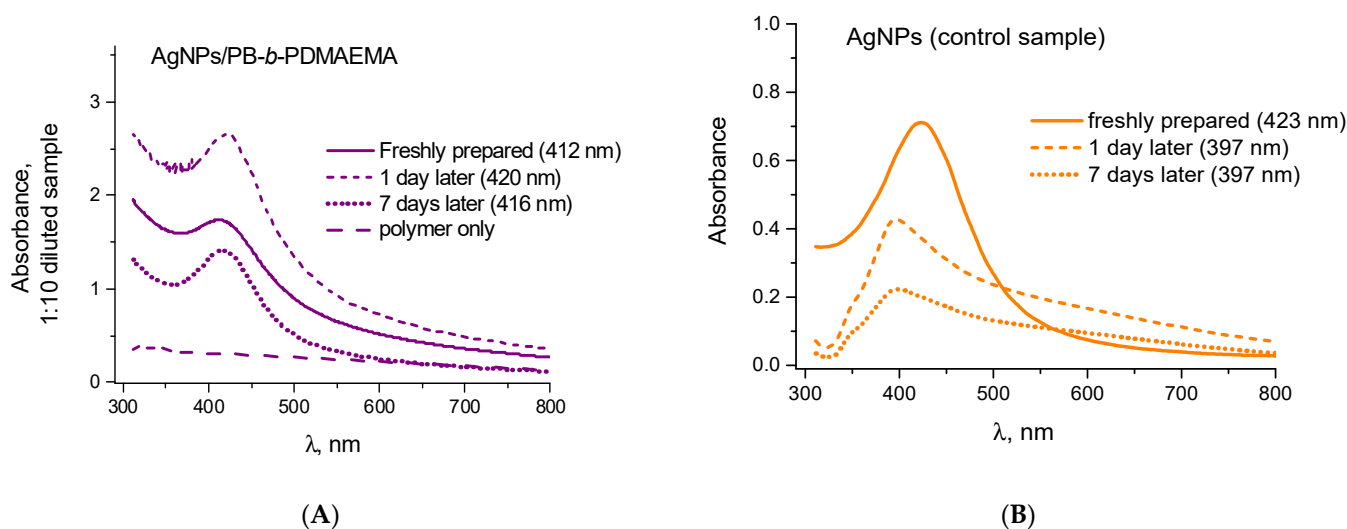


**Figure 1.** The time evolution of the UV–Vis spectra for the AgNPs prepared (A) in the presence and (B) in the absence of the PB-*b*-PDMAEMA micelles.

The TEM images of the AgNPs that were in situ templated on the PDMAEMA blocks of the PB-*b*-PDMAEMA micelles are demonstrated in Figure 2A. Two types of objects are clearly visible in the obtained images. Numerous small darker spots are undoubtedly attributed to the AgNPs while light grey round-shape structures, which are significantly weaker in contrast, are thought to represent PB-*b*-PDMAEMA micelles in a dry state. More TEM images of the prepared AgNPs/PB-*b*-PDMAEMA metallopolymer hybrids are given in Figure S2.

Furthermore, the AgNPs formed in the presence of the PB-*b*-PDMAEMA micelles were mostly spherical-like ones, which were separated from each other (Figure 2A). Although one cannot definitely see how the AgNPs are distributed within the PB-*b*-PDMAEMA micelles, they are most likely located in the external (periphery) part of the micelles, that is, in the micellar corona built up by PDMAEMA blocks. Importantly, the TEM image of the control sample of AgNPs, which were synthesized in the absence of the PB-*b*-PDMAEMA diblock copolymer, considerably differs from that taken for the AgNPs/PB-*b*-PDMAEMA sample. Indeed, only aggregated AgNPs are observed in this case, as shown in Figure S3. These results further confirm a considerable stabilization of the AgNPs in these metallopolymer hybrids.

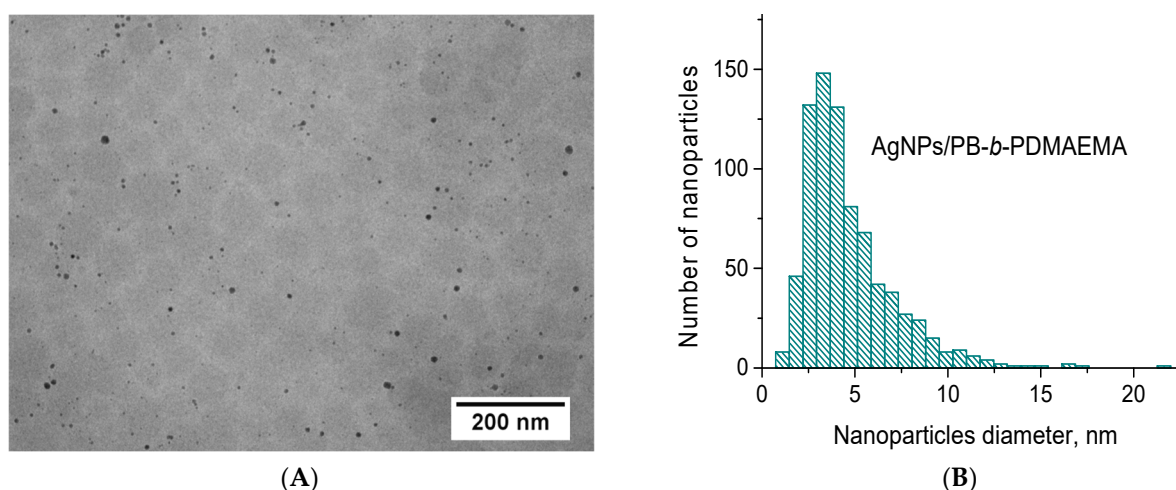


**Figure 2.** (A) The TEM image and (B) the corresponding size distributions of the AgNPs prepared in the presence of PB-*b*-PDMAEMA micelles.

As follows from Figure 2B, the size distribution of the AgNPs formed in the presence of the PB-*b*-PDMAEMA micelles was found to be rather narrow. Their mean diameter was calculated as  $4.6 \pm 2.5$  nm ( $n = 800$ ). Assuming that all of them are isotropic and possess a crystalline structure with the closest-packed Ag atoms that form a *face-centered cubic lattice*, one can evaluate the mean number of Ag atoms per NP. Indeed, the volume of a lattice cell for a silver face-centered cubic lattice ( $a = b = c = 0.4086$  nm) is  $V = 0.0682$  nm<sup>3</sup> with the number of Ag atoms per lattice cell of 4. Hence, one AgNP with a mean diameter of  $4.6 \pm 2.5$  nm contains approximately 2990 atoms. If we assume that Ag atoms form less-packed clusters, then one can calculate the same for a *simple cubic lattice* ( $a = b = c = 0.288$  nm, where 0.288 nm is a diameter of Ag atom). In this case, the volume of the lattice cell is  $V = 0.0239$  nm<sup>3</sup> with the number of Ag atoms per lattice cell of 1. Hence, one can evaluate approximately 2130 atoms per one AgNP with a mean diameter of  $4.6 \pm 2.5$  nm. Thus, one can consider 2990 and 2130 values as an upper-bound estimate and a lower-bound estimate for the number of Ag atoms per one AgNP, respectively.

Keeping in mind that the molar ratio of N:Ag was set to 20:1 (see Section 2.2 for the conditions applied for the synthesis of the AgNPs), one can easily calculate the concentration of AgNPs in the AgNPs/PB-*b*-PDMAEMA system as  $1.51 \times 10^{17}$  particles/L (assuming a crystalline structure of the AgNPs) or  $2.12 \times 10^{17}$  particles/L (assuming a cluster structure of the AgNPs). Dividing these values by the concentration of the PB-*b*-PDMAEMA micelles (independently determined by means of nanoparticle tracking analysis as  $3.7 \times 10^{16}$  micelles/L [29]), one can further evaluate the mean number of the AgNPs per one micelle. Hence, one PB-*b*-PDMAEMA micelle apparently contains between 4 and 6 AgNPs. It is worth noting that these evaluations are in very good agreement with the analysis of the obtained TEM images (Figure 2A), wherein 5–6 AgNPs per one PB-*b*-PDMAEMA micelle were counted.

A thermoresponsive behavior of the PB-*b*-PDMAEMA micelles and the prepared AgNPs/PB-*b*-PDMAEMA metallopolymer hybrids was revealed in our work by means of turbidimetry. The measurements were performed for 0.2 g/L solutions of each sample at a heating rate of 0.4 °C/min. A temperature-induced hydrophobization of the PDMAEMA blocks and the subsequent aggregation of the PB-*b*-PDMAEMA micelles resulted in a change in the transmittance of the samples (Figure 3A). The inflection points in the transmittance–temperature curves, which correspond to the onset temperature of the transmittance decrease, are defined herein as the onset temperature of the phase transition  $T_{PT}$ . As shown in Figure 3A, the transmittance curves demonstrate temperature-induced phase transition for both the PB-*b*-PDMAEMA micelles and for the AgNPs/PB-*b*-PDMAEMA metallopolymer hybrids, although the intensity of the process and the temperature ranges are remarkably different. Indeed, the  $T_{PT}$  for the PB-*b*-PDMAEMA

micelles was determined as 38 °C while the AgNPs/PB-*b*-PDMAEMA metallopolymer hybrids exhibit a higher  $T_{PT}$  of 52 °C (Figure 3A). Moreover, the phase transition in the latter case looks considerably less sharp and less pronounced. Apparently, the loading of PDMAEMA blocks with the AgNPs notably suppresses the temperature-induced phase transition. Furthermore, Figure 3B clearly demonstrates that the phase transition for the AgNPs/PB-*b*-PDMAEMA metallopolymer hybrids is completely reversible (at least, within the examined temperature cycle of 30 °C–60 °C–30 °C).

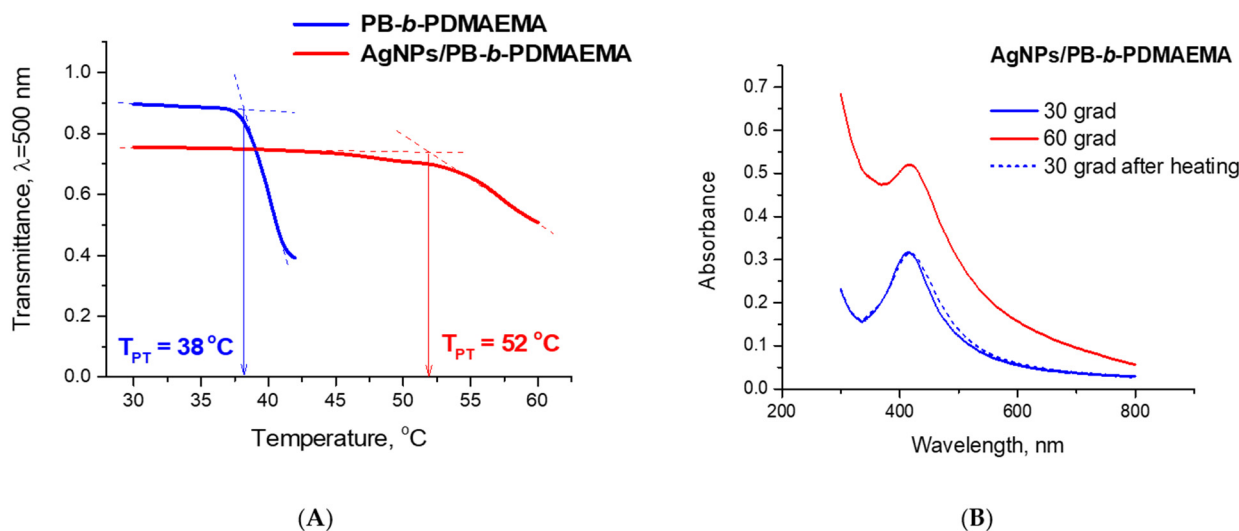


**Figure 3.** (A) Temperature-dependent changes in the transmittance of 0.2 g/L aqueous solutions of the PB-*b*-PDMAEMA micelles (blue line) and the AgNPs/PB-*b*-PDMAEMA hybrids (red line). (B) The UV-Vis spectra of 0.2 g/L aqueous solutions of the AgNPs/PB-*b*-PDMAEMA hybrids recorded at different temperatures. The pH values of all solutions were adjusted to pH 9 by 0.1 M NaOH.

Thus, a successful synthesis of the AgNPs on a PB-*b*-PDMAEMA micellar template was confirmed by means of UV-Vis spectroscopy and TEM, wherein the shape and size of the AgNPs were determined. We also demonstrated a reversible character of the temperature-induced phase separation for the AgNPs/PB-*b*-PDMAEMA metallopolymer hybrids. These findings allow us to expect a compulsory aggregation of the AgNPs upon a laser beam exposure of the AgNPs/PB-*b*-PDMAEMA samples. Indeed, the plasmonic heating of AgNPs is thought to result in a temperature-induced collapse of PDMAEMA blocks (coil-to-globule transition) and their aggregation, thereby initiating the approaching of the AgNPs and appearance of “hot spots”. As consequence, the SERS effect is to be observed.

### 3.2. SERS for the AgNPs Templated on the PB-*b*-PDMAEMA Micelles

To reveal a potential of the AgNPs/PB-*b*-PDMAEMA metallopolymer hybrids to exhibit the SERS effect, the AgNPs were labeled with 4-MPBA. As it forms a strong Ag-S bond, this compound can covalently bind to AgNPs. The covalent bond formation also leads to the appearance of intense peaks in the SERS spectrum of 4-MPBA that renders it an outstanding reporter for SERS experiments with AgNPs. Moreover, boronic acid itself can covalently bind to polyols, including carbohydrates and glycosylated proteins, which can be advantageously exploited for the diagnosis of diabetes, thereby emphasizing the biochemical relevance of 4-MPBA [39].

The chemical structure and the exemplary SERS spectrum of 4-MPBA with characteristic vibrations is shown in Figure S4. The most intense peaks of 4-MPBA are at 414, 992, 1018, 1070, 1178, and 1570  $\text{cm}^{-1}$ . The peak at 1070  $\text{cm}^{-1}$  is related to the in-plane benzene ring breathing mode coupled with the C-S stretching mode [40]. In further SERS experiments, the amplitude of this peak was used as an analytical signal.

To demonstrate the SERS effect for the AgNPs/PB-*b*-PDMAEMA metallopolymer hybrids, a drop of the AgNPs/PB-*b*-PDMAEMA sample labeled with 4-MPBA was deposited on aluminum foil and then an initial SERS spectrum was acquired first. After that, the sample was continuously exposed to laser beam for 1 min. Then, a second SERS spectrum was acquired under the same conditions. This procedure was repeated eight times so that the total time of laser exposition was equal to 8 min. Figure 4 demonstrates that a continuous laser exposure leads to a notable increase in the intensity of the SERS spectra, the increase being proportional to the exposure time. This result is thought to be a consequence of the local “hot spot” generation through a laser-induced collapse of PDMAEMA blocks (coil-to-globule transition) and their aggregation, followed by AgNPs approaching.

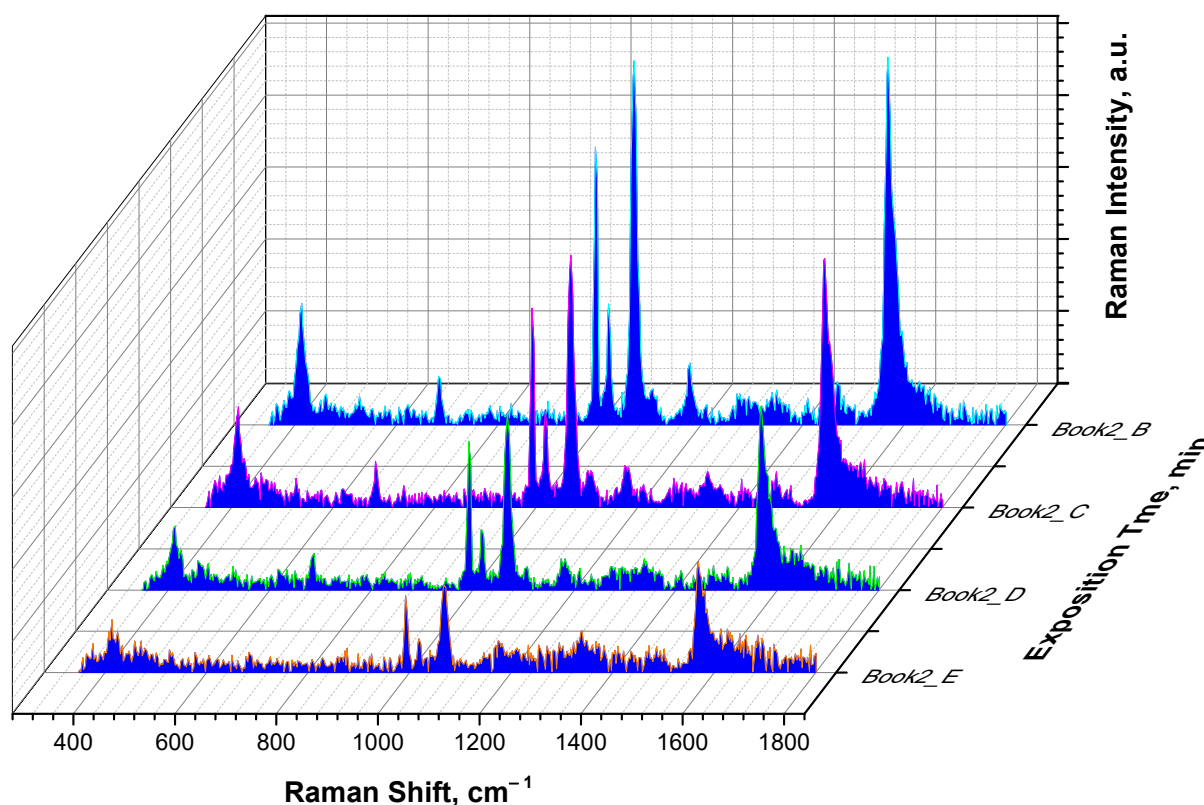


**Figure 4.** The evolution of the SERS spectra of the 10  $\mu\text{L}$  drop of the AgNPs/PB-*b*-PDMAEMA hybrid with 30  $\mu\text{M}$  of 4-MPBA at different exposure times: 0 min (orange line); 3 min (green line); 6 min (pink line); and 8 min (light blue line).

To prove whether the observed effect of the SERS intensity increase is due to a local laser exposure of the sample, a control experiment was performed, which started from recording the series of SERS spectra acquired in between five cycles of a 1 min laser exposure. Then, the laser was switched off, the drop of the sample was carefully mixed, and after that, one more SERS spectrum was recorded under the same conditions. As one can see from Figure 5, the intensity of the characteristic peak at 1070  $\text{cm}^{-1}$  drops back to the initial value. Indeed, exchanging the exposed sample volume by a portion of the fresh sample via stirring leads to a decrease in the intensity of the SERS spectrum back to the start point, thus confirming that the local laser exposure plays a key role in the observed increase in the SERS signal.

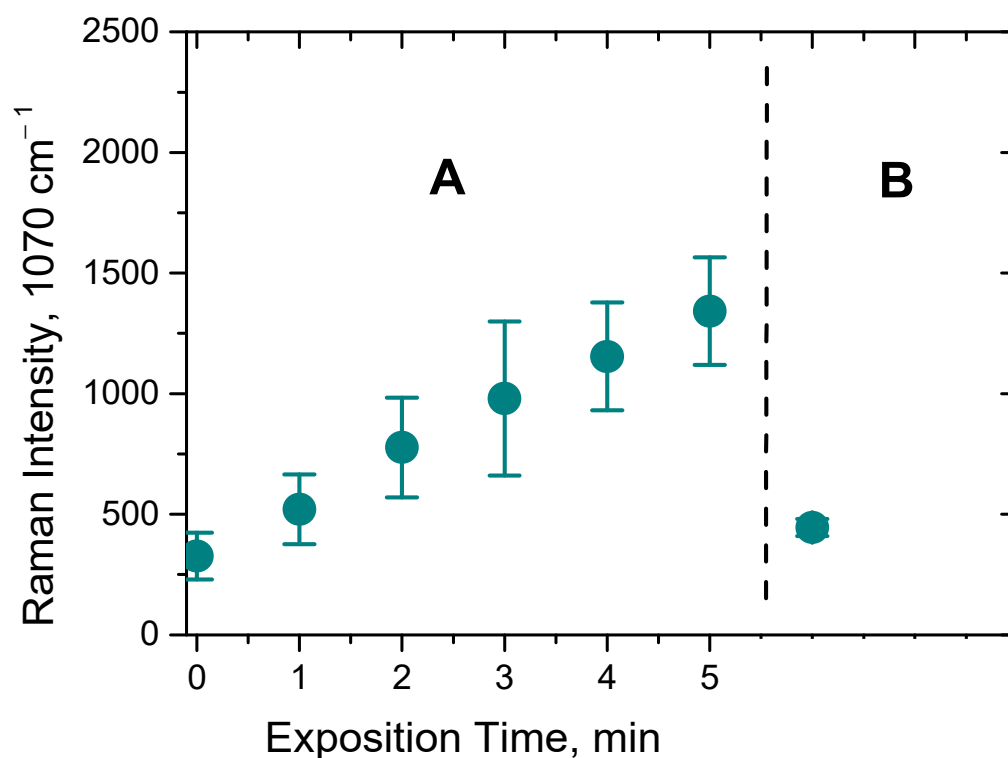


**Figure 5.** (A) The intensity increase in the 4-MPBA characteristic peak at  $1070\text{ cm}^{-1}$  upon 5 cycles of a local laser exposure of a drop of the AgNPs/PB-*b*-PDMAEMA hybrid labeled with 4-MPBA; (B) The intensity of the 4-MPBA characteristic peak at  $1070\text{ cm}^{-1}$  upon mixing a drop of the sample of the AgNPs/PB-*b*-PDMAEMA hybrid labeled with 4-MPBA. The data are presented as the mean  $\pm$  SD for three independent experiments.

Furthermore, we recorded the SERS spectra in the same manner at different 4-MPBA concentrations and compared the intensities of the characteristic peak at  $1070\text{ cm}^{-1}$  at different times of laser exposure. As one can see from Figure 6B–E, eight 1 min cycles of the continuous laser exposure lead to a notable increase in the start point, the endpoint, and the signal growth rate of the SERS signal intensity, the increase being proportional to the time of the laser exposure and to the concentration of 4-MPBA. A close to linear signal growth with the laser exposure is evident, although some deviations from linearity are found at the high concentrations of 4-MPBA. One can also note a concentration dependence of the initial SERS signal in the start point. This might be a consequence of a certain initial aggregation of the AgNPs, which could be induced by 4-MPBA upon its mixing with the AgNPs/PB-*b*-PDMAEMA sample. A control sample, which was measured in the absence of 4-MPBA, demonstrates no SERS signal (Figure 6A). One more control sample measured at  $30\text{ }\mu\text{M}$  of 4-MPBA in the absence of the AgNPs/PB-*b*-PDMAEMA metallopolymer hybrids shows no SERS signal either (data not shown). Here, the time of the laser exposure was limited to 8 min to avoid the significant evaporation of the sample. The evaporation of a  $10\text{ }\mu\text{L}$  drop was followed in a separate experiment and was found to be not exceeding 20% of the drop volume.

The endpoint intensities of the characteristic peak at  $1070\text{ cm}^{-1}$  were plotted against the concentration of 4-MPBA (Figure 6F). By this experiment, we demonstrated a potential benefit of such local triggering effects for the AgNPs/PB-*b*-PDMAEMA metallopolymer hybrids in the context of the SERS sensing applications. We think that the new approach considered herein could significantly broaden the applied range of SERS sensing, which could have possible applications in areas such as nanosensors for biologically relevant molecules.

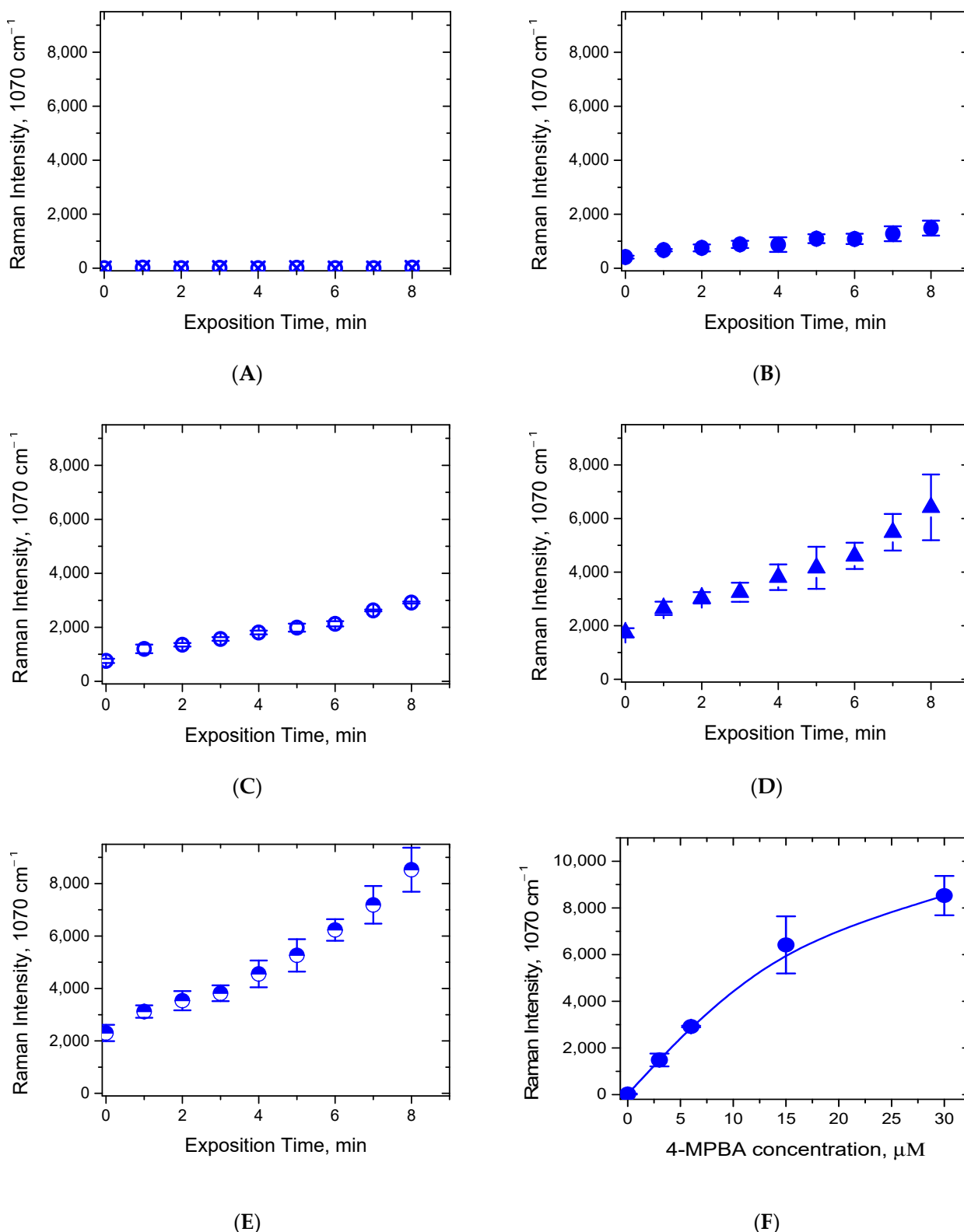


**Figure 6.** (A–E) The intensity increase in the 4-MPBA characteristic peak at 1070 cm<sup>-1</sup> upon 8 cycles of local laser exposure of a drop of the AgNPs/PB-*b*-PDMAEMA hybrid labeled with 4-MPBA at different 4-MPBA concentrations (A) 0 μM (control with water), (B) 3 μM, (C) 6 μM, (D) 15 μM, and (E) 30 μM; (F) the dependence of the intensity of characteristic peak at 1070 cm<sup>-1</sup> on 4-MPBA concentration plotted for the laser exposure time equal to 8 min. The data are presented as the mean ± SD for three independent experiments.

### 3.3. Theoretical Simulation of Sample Heating by a Laser Beam in SERS Experiments

To confirm that a laser exposure of the AgNPs/PB-*b*-PDMAEMA sample in the SERS experiments leads to heating that is sufficient for the temperature-induced collapse and aggregation of PDMAEMA blocks, a theoretical consideration of sample heating by a laser beam was carried out. The temperature distribution in a sample drop was simulated, based on the volume-specific heat source distribution resulting from the absorption of the laser light by AgNPs. The absorbance spectra (Figure 1A) of the diblock copolymer solutions with and without the AgNPs were used to determine the light absorption per unit volume. It was assumed that the extinction of a solution without the AgNPs resulted from the light scattering by PB-*b*-PDMAEMA micelles. Then, the difference between the extinctions of solutions with and without the AgNPs is expected to be exclusively due to light absorption in the AgNPs. Here, we neglected the own light scattering of the AgNPs since for the AgNPs with a size distribution as in our samples (Figure 2B), the average absorption cross-section is approximately an order of magnitude larger than the average scattering cross-section at  $\lambda = 532$  nm. To determine the volume-specific heat source distribution, the absorption coefficient of the AgNPs/PB-*b*-PDMAEMA sample (determined from the difference between the extinction spectra of the samples with and without the AgNPs) and the exponential attenuation of the laser intensity (determined from the entire extinction of the sample with the AgNPs) were taken into account.

Figure 7 shows the temperature increase distribution (relative to the room temperature) in a sample drop lying on an aluminum foil and in the surrounding media in the steady state. The maximum temperature increase in the sample was assessed as 37.7 K with respect to room temperature, which is sufficient for PDMAEMA blocks to collapse and aggregate as experimentally shown (Figure 3A). We assume that the SERS signal increase could be explained by the gradual temperature-induced transformation of the polymer in the steady temperature distribution (according to [19,20], the temperature-induced collapse time of thermoresponsive polymers might take approximately hundreds of seconds).

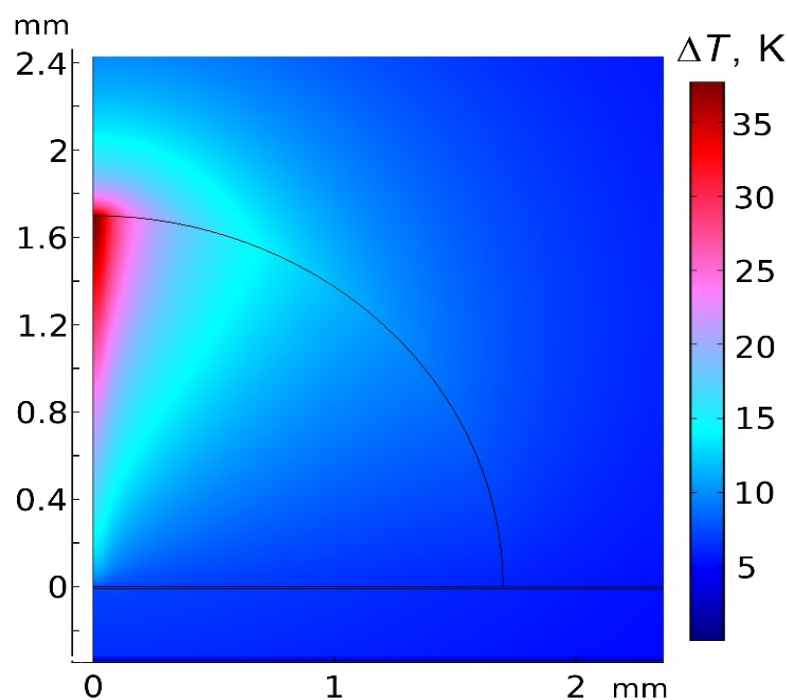


**Figure 7.** The simulated temperature increase distribution (with respect to the room temperature) resulting from laser heating in a sample drop (by a volume of 10  $\mu$ L) on a foil and in the surrounding air (in the axisymmetric geometry). The horizontal direction corresponds to the radial coordinate (the symmetry axis is perpendicular to the foil plane and coincides with the laser beam axis).

#### 4. Conclusions

In summary, we synthesized the AgNPs templated on the thermoresponsive PB-*b*-PDMAEMA micelles and showed a temperature-induced reversible phase transition of the prepared AgNPs/PB-*b*-PDMAEMA metallopolymer hybrids. With a SERS reporting probe (4-MPBA), we further revealed a laser-induced enhancement of a SERS signal observed under a constant local laser irradiation. The triggered SERS effect depends on the time of the laser exposure and on the concentration of 4-MPBA. The local heating of the AgNPs/PB-*b*-PDMAEMA sample in a laser spot is in good agreement with a performed theoretical consideration pointing to a temperature increase up to approximately 38 °C. A plasmonic heating of the AgNPs during the local laser exposure of the AgNPs/PB-*b*-PDMAEMA sample is thought to be responsible for the triggered SERS effect. Indeed, the plasmonic heating initiates a collapse of the PDMAEMA blocks and their gradual aggregation, which leads to the approaching of the AgNPs and generation of “hot spots”. However, an optical trapping effect (optical tweezers) that might appear as a result of a decreasing distance among the AgNPs as reported in [21] could also be a reasonable explanation.

We think that the smart stimuli-responsive metallopolymer hybrid materials reported herein could have promising applications in areas such as SERS nanosensors for the detection and quantification of biologically relevant molecules. At the same time, further optimization of the technique and the experimental conditions appears to be necessary to improve the approach and to increase the sensitivity, both of which will be subjects of future work.

**Supplementary Materials:** The following supporting information can be downloaded at: <https://www.mdpi.com/article/10.3390/bios12080628/s1>, Figure S1: The chemical structure of the PB-*b*-PDMAEMA (A) and the cryo-TEM micrograph of the PB-*b*-PDMAEMA micelles (B) in 50 mM sodium phosphate ( $c = 2.5$  g/L) at pH 7.0. Figure S2: The TEM images of the AgNPs/PB-*b*-PDMAEMA hybrids taken from different places of the sample at different magnification. Figure S3: The TEM image of the control AgNPs sample that was prepared under the same conditions in the absence of the PB-*b*-PDMAEMA micelles. Figure S4: The typical SERS spectrum of 4-MPBA with characteristic vibrations.

**Author Contributions:** Conceptualization, L.V.S.; methodology, L.V.S., N.L.N., I.N.K., A.M.M., A.I.I. and D.V.P.; validation, N.L.N., L.Y.F., T.Z.S., A.I.I. and D.V.P.; formal analysis, N.L.N., T.Z.S., L.Y.F., A.I.I. and D.V.P.; investigation, J.E., N.L.N. and L.Y.F.; resources, I.N.K. and F.H.S.; data curation, L.V.S., I.N.K. and A.M.M.; writing—original draft preparation, L.V.S., N.L.N. and A.I.I.; writing—review and editing, L.V.S., D.V.P. and F.H.S.; visualization, L.V.S., N.L.N., A.I.I. and T.Z.S.; supervision, L.V.S., D.V.P. and I.N.K.; project administration, L.V.S., F.H.S. and I.N.K.; funding acquisition, L.V.S., F.H.S. and I.N.K. All authors have read and agreed to the published version of the manuscript.

**Funding:** The synthesis of the AgNPs/PB-*b*-PDMAEMA hybrids used in this research was supported by the Russian Science Foundation (RSF, project no. 18-44-04011) and the Deutsche Forschungsgemeinschaft (DFG, SCHA1640/18-1) within a joint RSF-DFG grant. The TEM facilities of the Jena Center for Soft Matter (JCSM) were established with a grant from the German Research Council (DFG) and the European Fonds for Regional Development (EFRE). The physico-chemical characterization of the PB-*b*-PDMAEMA diblock copolymer and the AgNPs/PB-*b*-PDMAEMA hybrids was supported by the State Registration Topic “Modern Problems in Chemistry and Physical Chemistry of High Molecular Compounds” for 2021–2024 (no. AAAA-A21-121011990022-4). The SERS experiments were supported by the State Registration Topics “Molecular Design, Structure-Function Analysis and Regulation of Enzyme Systems, Cellular Structures, Bionanomaterials: Fundamental Basis and Applications in Technology, Medicine, Environmental Protection” for 2021–2024 (no. 121041500039-8), “Physical Chemistry of Bioanalytical Processes and Development of New Sensor Materials” (no. AAAA-A19-119071890024-8), and the M.V. Lomonosov Moscow State University Program of Development.

**Institutional Review Board Statement:** Not applicable.

**Informed Consent Statement:** Not applicable.

**Data Availability Statement:** Research data are not shared.

**Acknowledgments:** The authors thank Johannes B. Max for the technical assistance with TEM experiments.

**Conflicts of Interest:** The authors declare no conflict of interest.

## References

1. Cialla, D.; März, A.; Böhme, R.; Theil, F.; Weber, K.; Schmitt, M.; Popp, J. Surface-enhanced Raman spectroscopy (SERS): Progress and trends. *Anal. Bioanal. Chem.* **2012**, *403*, 27–54. [[CrossRef](#)] [[PubMed](#)]
2. Haynes, C.L.; McFarland, A.D.; Van Duyne, R.P. Surface-enhanced Raman spectroscopy. *Anal. Chem.* **2005**, *77*, 339A–346A. [[CrossRef](#)]
3. Asiala, S.M.; Schultz, Z.D. Characterization of hotspots in a highly enhancing SERS substrate. *Analyst* **2011**, *136*, 4472–4479. [[CrossRef](#)] [[PubMed](#)]
4. Brouers, F.; Blacher, S.; Lagarkov, A.; Sarychev, A.K. Theory of giant Raman scattering from semicontinuous metal films. *Phys. Rev. B—Condens. Matter Mater. Phys.* **1997**, *55*, 13234–13245. [[CrossRef](#)]
5. Guerrini, L.; Graham, D. Molecularly-mediated assemblies of plasmonic nanoparticles for Surface-Enhanced Raman Spectroscopy applications. *Chem. Soc. Rev.* **2012**, *41*, 7085–7107. [[CrossRef](#)]
6. Bell, S.E.J.; Sirimuthu, N.M.S. Surface-Enhanced Raman Spectroscopy as a Probe of Competitive Binding by Anions to Citrate-Reduced Silver Colloids. *J. Phys. Chem. A* **2005**, *109*, 7405–7410. [[CrossRef](#)]
7. Radziuk, D.; Grigoriev, D.; Zhang, W.; Su, D.; Möhwald, H.; Shchukin, D. Ultrasound-Assisted Fusion of Preformed Gold Nanoparticles. *J. Phys. Chem. C* **2010**, *114*, 1835–1843. [[CrossRef](#)]
8. Podoyntsyn, S.N.; Sorokina, O.N.; Nechaeva, N.L.; Yanovich, S.V.; Kurochkin, I.N. Surface-enhanced Raman spectroscopy in tandem with a gradient electric field from 4-mercaptophenylboronic acid on silver nanoparticles. *Microchim. Acta* **2020**, *187*, 566. [[CrossRef](#)]
9. Ding, T.; Rudrum, A.W.; Herrmann, L.O.; Turek, V.; Baumberg, J.J. Polymer-assisted self-assembly of gold nanoparticle monolayers and their dynamical switching. *Nanoscale* **2016**, *8*, 15864–15869. [[CrossRef](#)]
10. Manikas, A.C.; Aliberti, A.; Causa, F.; Battista, E.; Netti, P.A. Thermoresponsive PNIPAAm hydrogel scaffolds with encapsulated AuNPs show high analyte-trapping ability and tailored plasmonic properties for high sensing efficiency. *J. Mater. Chem. B* **2015**, *3*, 53–58. [[CrossRef](#)]
11. Nguyen, M.; Kanaev, A.; Sun, X.; Lacaze, E.; Lau-Truong, S.; Lamouri, A.; Aubard, J.; Felidj, N.; Mangeney, C. Tunable Electromagnetic Coupling in Plasmonic Nanostructures Mediated by Thermoresponsive Polymer Brushes. *Langmuir* **2015**, *31*, 12830–12837. [[CrossRef](#)] [[PubMed](#)]
12. Schild, H.G. Poly (N-isopropylacrylamide): Experiment, theory and application. *Prog. Polym. Sci.* **1992**, *17*, 163–249. [[CrossRef](#)]
13. Yin, P.G.; Chen, Y.; Jiang, L.; You, T.T.; Lu, X.Y.; Guo, L.; Yang, S. Controlled dispersion of silver nanoparticles into the bulk of thermosensitive polymer microspheres: Tunable plasmonic coupling by temperature detected by surface enhanced Raman scattering. *Macromol. Rapid Commun.* **2011**, *32*, 1000–1006. [[CrossRef](#)]
14. Dong, X.; Chen, S.; Zhou, J.; Wang, L.; Zha, L. Self-assembly of monodisperse composite microgels with bimetallic nanorods as core and PNIPAM as shell into close-packed monolayers and SERS efficiency. *Mater. Des.* **2016**, *104*, 303–311. [[CrossRef](#)]
15. Dong, X.; Zou, X.; Liu, X.; Lu, P.; Yang, J.; Lin, D.; Zhang, L.; Zha, L. Temperature-tunable plasmonic property and SERS activity of the monodisperse thermo-responsive composite microgels with core-shell structure based on gold nanorod as core. *Colloids Surf. A Physicochem. Eng. Asp.* **2014**, *452*, 46–50. [[CrossRef](#)]
16. Zheng, Y.; Soeriyadi, A.H.; Rosa, L.; Ng, S.H.; Bach, U.; Justin, J. Gooding, Reversible gating of smart plasmonic molecular traps using thermoresponsive polymers for single-molecule detection. *Nat. Commun.* **2015**, *6*, 8797. [[CrossRef](#)]
17. Elashnikov, R.; Mares, D.; Podzimek, T.; Švorčík, V.; Lyutakov, O. Sandwiched gold/PNIPAm/gold microstructures for smart plasmonics application: Towards the high detection limit and Raman quantitative measurements. *Analyst* **2017**, *142*, 2974–2981. [[CrossRef](#)]
18. Wu, Y.; Zhou, F.; Yang, L.; Liu, J. A shrinking strategy for creating dynamic SERS hot spots on the surface of thermosensitive polymer nanospheres. *Chem. Commun.* **2013**, *49*, 5025–5027. [[CrossRef](#)]
19. Hofkens, J.; Hotta, J.; Sasaki, K.; Masuhara, H.; Iwai, K. Molecular assembling by the radiation pressure of a focused laser beam: Poly(N-isopropylacrylamide) in aqueous solution. *Langmuir* **1997**, *13*, 414–419. [[CrossRef](#)]
20. Tsuboi, Y.; Nishino, M.; Sasaki, T.; Kitamura, N. Poly (N-isopropylacrylamide) Microparticles Produced by Radiation Pressure of a Focused Laser Beam: A Structural Analysis by Confocal Raman Microspectroscopy Combined with a Laser-Trapping Technique. *J. Phys. Chem. B* **2005**, *109*, 7033–7039. [[CrossRef](#)]
21. Aibara, I.; Mukai, S.; Hashimoto, S. Plasmonic-Heating-Induced Nanoscale Phase Separation of Free Poly(N-isopropylacrylamide) Molecules. *J. Phys. Chem. C* **2016**, *120*, 17745–17752. [[CrossRef](#)]
22. Yeshchenko, O.A.; Bartenev, A.O.; Naumenko, A.P.; Kutsevol, N.V.; Harahuts, I.I.; Marinin, A.I. Laser-driven aggregation in dextran-graft-PNIPAM/silver nanoparticles hybride nanosystem: Plasmonic effects. *Ukr. J. Phys.* **2020**, *65*, 254–267. [[CrossRef](#)]

23. Plamper, F.A.; Schmalz, A.; Ballauff, M.; Müller, A.H.E. Tuning the Thermoresponsiveness of Weak Polyelectrolytes by pH and Light: Lower and Upper Critical-Solution Temperature of Poly(N,N-dimethylaminoethyl methacrylate). *J. Am. Chem. Soc.* **2007**, *129*, 14538–14539. [[CrossRef](#)]
24. Plamper, F.A.; Ruppel, M.; Schmalz, A.; Borisov, O.; Ballauff, M.; Müller, A.H.E. Tuning the Thermoresponsive Properties of Weak Polyelectrolytes: Aqueous Solutions of Star-Shaped and Linear Poly(N,N-dimethylaminoethyl Methacrylate). *Macromolecules* **2007**, *40*, 8361–8366. [[CrossRef](#)]
25. Sigolaeva, L.V.; Günther, U.; Pergushov, D.V.; Gladyr, S.Y.; Kurochkin, I.N.; Schacher, F.H. Sequential pH-dependent adsorption of ionic amphiphilic diblock copolymer micelles and choline oxidase onto conductive substrates: Toward the design of biosensors. *Macromol. Biosci.* **2014**, *14*, 1039–1051. [[CrossRef](#)] [[PubMed](#)]
26. Sigolaeva, L.V.; Konyakhina, A.Y.; Pergushov, D.V.; Kurochkin, I.N. Electrochemical Biosensor Based on Nanosized Polymer-Enzyme Films Composed of Linear Poly(N,N-Dimethylaminoethyl Methacrylate) and Choline Oxidase. *Moscow Univ. Chem. Bull.* **2021**, *76*, 334–342. [[CrossRef](#)]
27. Sigolaeva, L.V.; Pergushov, D.V.; Synatschke, C.V.; Wolf, A.; Dewald, I.; Kurochkin, I.N.; Fery, A.; Müller, A.H.E. Co-assemblies of micelle-forming diblock copolymers and enzymes on graphite substrate for an improved design of biosensor systems. *Soft Matter* **2013**, *9*, 2858–2868. [[CrossRef](#)]
28. Makhaeva, G.F.; Rudakova, E.V.; Sigolaeva, L.V.; Kurochkin, I.N.; Richardson, R.J. Neuropathy target esterase in mouse whole blood as a biomarker of exposure to neuropathic organophosphorus compounds. *J. Appl. Toxicol.* **2016**, *36*, 1468–1475. [[CrossRef](#)]
29. Shumyantseva, V.V.; Sigolaeva, L.V.; Agafonova, L.E.; Bulko, T.V.; Pergushov, D.V.; Schacher, F.H.; Archakov, A.I. Facilitated biosensing via direct electron transfer of myoglobin integrated into diblock copolymer/multi-walled carbon nanotube nanocomposites. *J. Mater. Chem. B* **2015**, *3*, 5467–5477. [[CrossRef](#)]
30. Sigolaeva, L.V.; Bulko, T.V.; Konyakhina, A.Y.; Kuzikov, A.V.; Masamrekh, R.A.; Max, J.B.; Köhler, M.; Schacher, F.H.; Pergushov, D.V.; Shumyantseva, V.V. Rational design of amphiphilic diblock copolymer/MWCNT surface modifiers and their application for direct electrochemical sensing of DNA. *Polymers* **2020**, *12*, 1514. [[CrossRef](#)]
31. Shumyantseva, V.V.; Agafonova, L.E.; Bulko, T.V.; Kuzikov, A.V.; Masamrekh, R.A.; Yuan, J.; Pergushov, D.V.; Sigolaeva, L.V. Electroanalysis of Biomolecules: Rational Selection of Sensor Construction. *Biochemistry* **2021**, *86*, S140–S151. [[CrossRef](#)] [[PubMed](#)]
32. Shumyantseva, V.V.; Bulko, T.V.; Kuzikov, A.V.; Masamrekh, R.A.; Konyakhina, A.Y.; Romanenko, I.; Max, J.B.; Köhler, M.; Gilep, A.A.; Usanov, S.A.; et al. All-electrochemical nanocomposite two-electrode setup for quantification of drugs and study of their electrocatalytical conversion by cytochromes P450. *Electrochim. Acta* **2020**, *336*, 135579. [[CrossRef](#)]
33. Shumyantseva, V.V.; Bulko, T.V.; Tikhonova, E.G.; Sanzhakov, M.A.; Kuzikov, A.V.; Masamrekh, R.A.; Pergushov, D.V.; Schacher, F.H.; Sigolaeva, L.V. Electrochemical studies of the interaction of rifampicin and nanosome/rifampicin with dsDNA. *Bioelectrochemistry* **2021**, *140*, 107736. [[CrossRef](#)] [[PubMed](#)]
34. Schallon, A.; Synatschke, C.V.; Pergushov, D.V.; Jérôme, V.; Müller, A.H.E.; Freitag, R. DNA Melting Temperature Assay for Assessing the Stability of DNA Polyplexes Intended for Nonviral Gene Delivery. *Langmuir* **2011**, *27*, 12042–12051. [[CrossRef](#)]
35. Raup, A.; Wang, H.; Synatschke, C.V.; Jérôme, V.; Agarwal, S.; Pergushov, D.V.; Müller, A.H.E.; Freitag, R. Compaction and transmembrane delivery of pDNA: Differences between l-PEI and two types of amphiphilic block copolymers. *Biomacromolecules* **2017**, *18*, 808–818. [[CrossRef](#)] [[PubMed](#)]
36. Ou, Y.; Wang, L.Y.; Zhu, L.W.; Wan, L.S.; Xu, Z.K. In-situ immobilization of silver nanoparticles on self-assembled honeycomb-patterned films enables surface-enhanced raman scattering (SERS) substrates. *J. Phys. Chem. C* **2014**, *118*, 11478–11484. [[CrossRef](#)]
37. Zhou, J.; Zha, X.; Chen, X.; Ma, J.  $\beta$ -Cyclodextrin-g-Poly(2-(dimethylamino) ethyl methacrylate) as the Stabilizer and Reductant to Prepare Colloid Silver Nanoparticles in situ. *Indian J. Pharm. Educ. Res.* **2017**, *51*, 543–550. [[CrossRef](#)]
38. Sun, H.; Gao, Z.; Yang, L.; Gao, L.; Lv, X. Synthesis and characterization of novel four-arm star PDMAEMA-stabilized colloidal silver nanoparticles. *Colloid Polym. Sci.* **2010**, *288*, 1713–1722. [[CrossRef](#)]
39. Nechaeva, N.L.; Boginskaya, I.A.; Ivanov, A.V.; Sarychev, A.K.; Eremenko, A.V.; Ryzhikov, I.A.; Lagarkov, A.N.; Kurochkin, I.N. Multiscale flaked silver SERS-substrate for glycosylated human albumin biosensing. *Anal. Chim. Acta* **2020**, *1100*, 250–257. [[CrossRef](#)]
40. Sun, F.; Bai, T.; Zhang, L.; Ella-Menye, J.-R.; Liu, S.; Nowinski, A.K.; Jiang, S.; Yu, Q. Sensitive and Fast Detection of Fructose in Complex Media via Symmetry Breaking and Signal Amplification Using Surface-Enhanced Raman Spectroscopy. *Anal. Chem.* **2014**, *86*, 2387–2394. [[CrossRef](#)]